DNA Repair xxx (2010) xxx–xxx

Contents lists available at ScienceDirect

DNA Repair

journal homepage: www.elsevier.com/locate/dnarepair

A semi-automated non-radioactive system for measuring recovery of RNA synthesis and unscheduled DNA synthesis using ethynyluracil derivatives

Yuka Nakazawa [a], Shunichi Yamashita [a,1], Alan R. Lehmann [b,1], Tomoo Ogi [a,*]

[a] Department of Molecular Medicine, Atomic Bomb Disease Institute, Graduate School of Biomedical Sciences, Nagasaki University, 1-12-4, Sakamoto, Nagasaki 852-8523, Japan
[b] Genome Damage and Stability Centre, University of Sussex, Falmer, Brighton BN1 9RQ, United Kingdom

ARTICLE INFO

Article history:
Received 27 November 2009
Received in revised form 22 January 2010
Accepted 23 January 2010
Available online xxx

Keywords:
Nucleotide excision repair (NER)
Transcription-coupled repair (TCR)
Recovery of RNA synthesis (RRS)
Unscheduled DNA synthesis (UDS)
Xeroderma pigmentosum (XP)
Cockayne syndrome (CS)

ABSTRACT

Nucleotide excision repair (NER) removes the major UV-photolesions from cellular DNA. In humans, compromised NER activity is the cause of several photosensitive diseases, one of which is the skin-cancer predisposition disorder, xeroderma pigmentosum (XP). Two assays commonly used in measurement of NER activity are 'unscheduled DNA synthesis (UDS)', and 'recovery of RNA synthesis (RRS)', the latter being a specific measure of the transcription-coupled repair sub-pathway of NER. Both assays are key techniques for research in NER as well as in diagnoses of NER-related disorders. Until very recently, reliable methods for these assays involved measurements of incorporation of radio-labeled nucleosides. We have established non-radioactive procedures for determining UDS and RRS levels by incorporation of recently developed alkyne-conjugated nucleoside analogues, 5-ethynyl-2′-deoxyuridine (EdU) and 5-ethynyuridine (EU). EdU and EU are respectively used as alternatives for ^{3}H-thymidine in UDS and for ^{3}H-uridine in RRS. Based on these alkyne-nucleosides and an integrated image analyser, we have developed a semi-automated assay system for NER-activity. We demonstrate the utility of this system for NER-activity assessments of lymphoblastoid samples as well as primary fibroblasts. Potential use of the system for large-scale siRNA-screening for novel NER defects as well as for routine XP diagnosis are also considered.

1. Introduction

Genetic information stored in DNA is continuously threatened by various types of DNA damaging activity. A failure of DNA repair in living cells induces genomic instability, and may eventually result in cancer and other pathological consequences [1].

Xeroderma pigmentosum (XP) and Cockayne syndrome (CS) are autosomal recessive photosensitive genodermatoses. XP-patients show sunlight-induced pigmentation changes and skin-cancer predisposition, and in some cases neurological degeneration and mental retardation. CS patients are not susceptible to skin carcinogenesis, but, in addition to sun sensitivity, they show dwarfism, severe mental retardation, microcephaly, developmental disorders, and premature aging [2–4]. Most XP and all CS cases are associated with a deficiency in nucleotide excision repair (NER), which deals with major UV-photolesions as well as many chemical DNA adducts [5,6]. There are two sub-pathways of NER. Global genome repair (GGR) is a relatively slow process that removes damage throughout the genome [7]. Transcription-coupled repair (TCR) is a more rapid process that removes damage specifically from the transcribed strand of genes that are being actively transcribed [8].

XP results from defects in one of eight genes, *XPA* through *G* and variant, whereas two genes, *CSA* and *CSB*, are responsible for CS. The XP A-G proteins are involved in different steps of NER. Recognition of the damage in GGR is mediated by the XPE and XPC proteins. The next step is opening out of the damaged region of DNA by TFIIH, which contains the XPD and XPB proteins and utilizes the helicase activity of XPD and the ATPase activity of XPB. After verification of the damage by XPA, the DNA is cleaved on the 5′ side of the damage by XPF and its partner protein ERCC1, and on the 3′ side by XPG. The damaged section is then removed and replaced by DNA polymerases, ligases and their accessory proteins.

TCR differs from GGR in the initial damage recognition stage. In TCR, stalling of the RNA polymerase at the lesion is the initiating signal, and results in recruitment of the CSB and CSA proteins. The role of these proteins is to recruit the later NER proteins and various chromatin remodeling proteins to allow the subsequent steps of NER to take place. The roles of TFIIH, XPA, F and G are the same in TCR and GGR. Thus CS is associated with specific defects in TCR, whereas XP-patients are defective in GGR alone (XPC and E) or in both GGR and TCR.

Abbreviations: EdU, 5-ethynyl-2′-deoxyuridine; EU, 5-ethynyuridine.

* Corresponding author. Tel.: +81 95 819 7103; fax: +81 95 819 7104.
E-mail address: togi@nagasaki-u.ac.jp (T. Ogi).

[1] These authors contributed equally to this work.

1568-7864/$ – see front matter © 2010 Elsevier B.V. All rights reserved.
doi:10.1016/j.dnarep.2010.01.015

Trichothiodystrophy (TTD) is a third disorder associated, in about 50% of cases, with defects in NER. In these cases, most are defective in *XPD*, a few in *XPB* and a few in a third gene *TTDA*. The products of these three genes are all components of TFIIH, which has independent roles in NER and in transcription. It is thought that mutations affecting the NER function result in XP, whereas those affecting transcription as well result in TTD. A few patients in the XPB, D and G groups have the combined features of XP and CS.

Diagnosis of NER-related-disorders as well as NER research typically involves determining the level of nucleotide incorporation associated with DNA repair activity [9,10]. GGR contributes 90–95% of NER and can be assessed by damage-induced, non-S-phase, DNA repair synthesis activity, termed unscheduled DNA synthesis (UDS) [9]. Patients with XP (except for the variant form, which is deficient in the translesion synthesis DNA polymerase, polη [11]), XP combined with CS (XP/CS), and NER-deficient TTD, are GGR-defective and can be diagnosed by determining UDS levels. TCR can be readily measured by 'recovery of RNA synthesis (RRS)' levels after DNA damaging treatment. UV-irradiation results in a decrease in RNA synthesis rates, which recover rapidly in normal cells, largely as a consequence of TCR [10]. In CS cells, which lack TCR, RNA synthesis does not recover and remains at a low level.

In XP-diagnostic laboratories, 254 nm UVC-irradiation is commonly used for inducing DNA damage; radio-labeled nucleosides, ^{3}H-thymidine and ^{3}H-uridine, have been generally used to measure UDS and RRS, respectively [9,10]. In both these assays, nuclear silver grain counting following autoradiography has been established as an accurate and sensitive but time-consuming and laborious technique, while direct liquid scintillation counting of acid-insoluble DNA or RNA is a quicker but less quantitative method [12].

We have recently described a non-radioactive method for UDS measurement that entails incorporation of an alkyne-conjugated thymidine analogue, 5-ethynyl-2′-deoxyuridine (EdU) [13], in combination with a direct fluorescent azide-coupling reaction using commercially available reagents (*Invitrogen*) [14]. This method provides a rapid and accurate alternative to the autoradiography-based assay; however, the method has so far been limited to determining GGR-activity and XP diagnosis as, until very recently, only a deoxy- form of the alkyne-nucleosides was available. Although this procedure obviates the need for labor-intensive autoradiographic procedures, our published procedure still uses manual analyses of individual coverslips, which is a potential disadvantage for routine diagnoses or screening-based operations.

Here we report the development of a semi-automated assay system for NER activity that is applicable to both UDS and RRS measurements using EdU and the more recently available 5-ethynyluridine (EU) [15]. The EU-based RRS assay complements our recently reported EdU-based UDS assay. We have employed improved protocols suitable for plastic 96-well plates and GE's '*In-Cell-Analyzer*'—an automated plate scanner equipped with a fluorescent microscope and a CCD camera. We demonstrate that the technique is compatible with lymphoblastoid samples and is also applicable to large-scale siRNA-screening projects.

2. Materials and methods

2.1. Cell strains and cultures

Normal 1BR [16] and 48BR [16], XP-patient-derived XP12BR (XP-D) [13], XP15BR (XP-A) [17], XP13BR (XP-C) [13], XP21BR (XP-C, this study) and XP20BE (XP-G) [18], and CS-patient-derived CS16PV (CS-A, *Miria Stefanini, personal communication*), CS20PV (CS-B, *Miria Stefanini, personal communication*) and CS10LO (CS-B) [19] cells were human primary fibroblasts. Normal 277 and 701 (both purchased from RIKEN), and XP-patient-derived XPL5 (XP-V) [20] and XPL15OS (XP-A) [20] are EBV-immortalised B-lymphoblastoids (LCLs). Fibroblasts and LCLs were cultured in respectively Dulbecco's Modified Eagle Medium (DMEM) and RPMI1640, both supplemented with 10% fetal calf serum (FCS) (Gibco-BRL) and penicillin–streptomycin (Wako).

2.2. UDS assay with incorporation of ethynyldeoxyuridine (EdU) and automation using the In-Cell-Analyzer

5-Ethynyl-2′-deoxyuridine (EdU) is available from *Invitrogen* [14]. To optimise UV-induced UDS by EdU incorporation and its measurement in microtiter plates with the *In-Cell-Analyzer*, effects of UV-dose, EdU concentration and incubation period, fluorodeoxyuridine (FdU), and fixation, permeabilisation and staining conditions were examined. 48BR cells were plated at confluent density in 96-well plastic microtiter plates (Falcon) and cultured for 16 h in DMEM supplemented with 10% FCS. Cells were washed with PBS, followed by irradiation with a range of doses (5–40 J/m^2) of UVC (254 nm, 50 μW/cm^2). After UV-irradiation, cells were immediately incubated for different time-periods (0.5–4 h) in serum-free DMEM supplemented with various concentrations of EdU (2.5–20 μM), and additionally supplemented with or without 1 μM FdU (*SIGMA*). Serum-free medium was used as serum often contains thymidine, which competes with EdU for incorporation into DNA. Cells were then washed with PBS, followed by fixation and permeabilisation. We examined two different fixation protocols: for 1-step fixation, cells were fixed and permeabilised in PBS containing 2% paraformaldehyde, 0.5% triton X-100, and 300 mM sucrose for 20 min on ice; for 2-step fixation, cells were fixed for 10 min on ice with PBS containing 3.7% paraformaldehyde, followed by permeabilisation with 0.5% triton X-100 in PBS for 5 min on ice. After extensive washing with PBS, cells were blocked for 30 min with 10% FCS in PBS at room temperature. To diminish background signal, we established the following improved azide-coupling staining protocol. Cells were incubated for 1 h with 25 μM Alexa Fluor 488-azide (*Invitrogen*) in freshly prepared 50 mM Tris–HCl (TBS) (pH 7.3), supplemented with 4 mM $CuSO_4$ and 10 mM sodium ascorbate, followed by extensive washing with PBST (0.05% Tween20). Cells were then incubated with 20 ng/ml DAPI in PBS for 20 min, and twice washed with PBST, followed by fixation in PBS containing 3.7% paraformaldehyde for 20 min.

We found that 20 J/m^2 UVC-irradiation, followed by 5 μM EdU incubation for 4 h without FdU supplement, and the 1-step fixation protocol was the optimal condition for the UDS assay on plastic 96-well plates. This condition was used for all experiments unless otherwise stated.

Image acquisition and data processing were automated using GE's *In-Cell-Analyzer* system: plates were scanned with a CCD-camera-equipped scanning microscope, and captured images were directly processed using the automated *Developer* software programmed for detection of nuclei (DAPI staining), measurements of the fluorescent intensity (Alexa Fluor 488 staining), and subtraction of background signals calculated from the fluorescent intensity of circumference of nuclei. All non-S-phase cells in a single captured field (60–70 cells) were evaluated, and the median fluorescence density values of discrete nuclei were calculated from the pixels contained in each nucleus. Data points presented in the figures are the averages calculated from ten different fields. *Developer Toolbox* scripts describing the assay protocols are available from the authors.

Please cite this article in press as: Y. Nakazawa, et al., A semi-automated non-radioactive system for measuring recovery of RNA synthesis and unscheduled DNA synthesis using ethynyluracil derivatives, DNA Repair (2010), doi:10.1016/j.dnarep.2010.01.015

2.3. Non-radioactive RRS assay by incorporation of ethynyluridine (EU) using the In-Cell-Analyzer

5-Ethynyluridine (EU) is available from *Invitrogen* [15]. To optimize RRS measurement by EU incorporation using plastic plates and the *In-Cell-Analyzer*, we again analysed the effects of various parameters. 48BR cells were plated at confluent density on 96-well plastic microtiter plates and cultured for 16 h in DMEM supplemented with 10% FCS. Cells were washed with PBS, followed by irradiation with a range of doses (5–20 J/m^2) of UVC. After UV-irradiation, cells were incubated for different time-periods (0–24 h) for RNA synthesis recovery in DMEM supplemented with 1% FCS. Cells were then immediately incubated for different time-periods (0.5–4 h) in serum-free DMEM supplemented with various concentrations of EU (50–1000 μM). Cells were then washed with PBS, followed by fixation and permeabilisation by the two different protocols, and azide-coupling reaction and DAPI staining as described above.

We found that 5 J/m^2 UVC-irradiation, followed by 4 h incubation for RNA synthesis recovery and 2 h labeling in media supplemented with 100 μM EU, and the 1-step fixation protocol was the optimal condition for the RRS assay on plastic 96-well plates. This condition was used for all experiments unless otherwise stated.

Image acquisition and data processing were automated using the *In-Cell-Analyzer* and the *Developer* software as described above. All cells in a single captured field were evaluated, and the median fluorescence density values of discrete nuclei were calculated from the pixels contained in each nucleus. Data points presented in the text are the averages calculated from ten different fields.

2.4. EdU-based UDS assay on lymphoblastoid samples

EBV-immortalised lymphoblastoid cells (LCLs) were cultured in RPMI1640 supplemented with 1% FCS (low-serum media) for 72 h prior to the experiments. This step is needed to minimise the number of cells in S-phase as DNA replicative synthesis significantly interferes with UDS signals in LCL samples. We tried different UV-doses (5–20 J/m^2), EdU concentrations (5–10 μM) and incubation time-periods (1–4 h), and fixation and permeabilisation protocols (data not shown), and found that the following condition is optimal for the UDS assay for LCL samples. Cells were centrifuged, suspended in PBS and UVC-irradiated (20 J/m^2) in non-tissue-culture-treated plastic dishes, followed by 1 h incubation in serum-free RPMI1640 supplemented with 10 μM EdU. After washing with PBS, cells were fixed and permeabilised in PBS containing 2% paraformaldehyde, 0.5% triton X-100, and 300 mM sucrose for 20 min on ice. Cells were then blocked for 30 min with 10% FCS in PBS at room temperature. Azide-coupling and DAPI staining were performed as described above, but all done in eppendorf tubes and 0.5 mM EDTA was included in all steps after the azide-coupling reaction. Processed cells were finally suspended in PBS supplemented with 0.5 mM EDTA, followed by cytospin-centrifugation at 1500 rpm for 2 min using multi-chamber cytofunnels (*Thermo*). Image acquisition and data processing were automated using the *In-Cell-Analyzer* system as described above.

2.5. RNA interference

Pre-designed siRNA oligos targeting for XP- and non-NER-related repair genes, and scrambled non-targeting controls were *the MISSION siRNA* purchased from *SIGMA* (the siRNA oligo sequences can be obtained from the authors upon request). siRNA transfection was performed using Xtream gene (*Roche*) transfection reagent according to the manufacturer's instruction. 10 nM of siRNA oligos were transfected in suspension, followed by one additional transfection cycle 24 h after the first transfection. UDS and RRS assays were performed 48 h after the first siRNA transfection. Knockdown efficiencies were confirmed by western blot.

3. Results

3.1. Development of an automated EdU-based UDS assay system using the In-Cell-Analyzer

We first optimised the EdU-based UDS assay conditions for the automated system (Fig. 1A). 48BR normal human primary fibroblasts were seeded into 96-well plates. Cells were then UVC (245 nm) irradiated with a range of doses, followed by incubation for different time-periods with serum-free media containing various concentrations of EdU, with or without the thymidylate synthetase inhibitor, fluorodeoxyuridine (FdU) (Fig. 1B–E). Incorporated EdU was detected by the Alexa Fluor 488-azide-coupling reaction using a modified coupling-buffer after permeabilisation of the cells using two different protocols (details described in Section 2). 96-well plates were then processed by the *In-Cell-Analyzer*. We were able to detect DNA damage-dependent EdU incorporation, which denotes UDS activity, in fibroblasts cultured on plastic-96-well plates, as previously observed in coverslip-based experiments (Fig. 1B). DAPI staining clearly enabled the detection of nuclei, which is needed for cell-cycle determination as well as for the automated nuclear fluorescent measurements (Fig. 1A and B); though we noted that the background fluorescent intensity was relatively higher than in the coverslip-based assay (data not shown), an appropriate background subtraction process, which is also a feature of the software (details described in Section 2, Fig. 1A), clearly diminished interference of unwanted fluorescent signals inside the nuclei (data not shown). We found that the EdU concentration did not significantly affect the UDS-specific nuclear fluorescent intensity levels over the range examined (Fig. 1C). A supplement of FdU contributed only slightly to the UDS specific EdU incorporation, whereas the permeabilisation processes significantly affected the fluorescent intensity (Fig. 1D). As we previously demonstrated [13], UDS dependent EdU incorporation was increased in proportion to UV-dose and incubation time period (Fig. 1E). We found that 10–20 J/m^2 UVC-irradiation, 5 μM EdU for 4 h labeling, and the one-step fix and permeabilisation process, are the optimum conditions for the EdU assay with the automated system.

3.2. Rapid assessment of GGR-deficiency in XP cells by the semi-automated UDS assay

We next assessed the UDS levels of several NER-deficient fibroblasts and normal controls. To evaluate the reproducibility and variation of the UDS levels assayed in plastic 96-well plates, each cell line was plated in quintuplicate and assayed as shown in Fig. 2A. Satisfyingly, plate-to-plate variation (data not shown) as well as well-to-well variation were both very small (compare bars 1–5, and 8–12 in each panel), indicating that the assay is very reproducible. We noted that the UDS levels of normal fibroblasts from five different individuals assayed in this system varied between 96 and 102% of 48BR cells (Fig. 2B and C, and data not shown); this variation was significantly smaller than that obtained with different assays based on cells plated on coverslips using either autoradiography or EdU incorporation [13]. We further determined the UDS levels of typical NER-deficient cell lines; as shown in Fig. 2D–G, severe NER-deficient XP cell lines, XP15BR (XP-A) and XP20BE (XP-G), showed no detectable UDS (Fig. 2D and E), whereas intermediate NER-deficient XP12BR (XP-D) and XP13BR (XP-C) cell lines elicited weak but statistically significant UDS activities (Fig. 2F and G).

Please cite this article in press as: Y. Nakazawa, et al., A semi-automated non-radioactive system for measuring recovery of RNA synthesis and unscheduled DNA synthesis using ethynyluracil derivatives, DNA Repair (2010), doi:10.1016/j.dnarep.2010.01.015

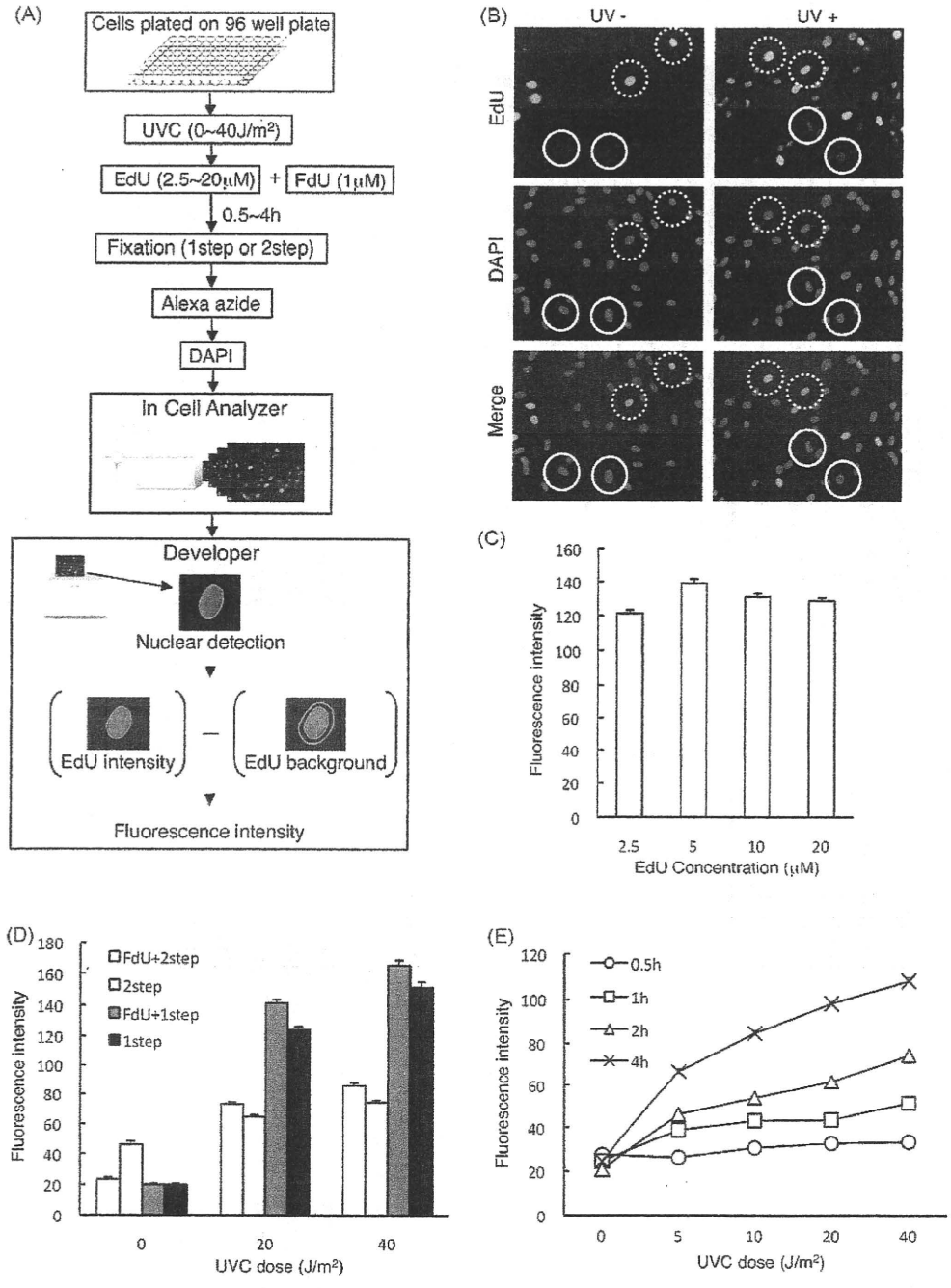

Fig. 1. EdU-based semi-automated UDS assay using the *In-Cell-Analyzer*. (A) An experimental scheme for the UDS assay. Cells were plated on plastic 96-well plates, UVC-irradiated (254 nm) with a range of doses (0–40 J/m²), followed by incubation for different time-periods (0.5–4 h) in serum-free media supplemented with various concentrations of EdU (2.5–20 μM), and additionally supplemented with or without 1 μM FdU. Fixation (1- or 2-step), conjugation of Alexa Fluor 488-azide to the incorporated EdU, and nuclear DAPI staining are described in Section 2. Image acquisition and data processing were automated using GE's *In-Cell-Analyzer* system. (B) Typical UDS images captured by the *In-Cell-Analyzer*. Normal 48BR cells were cultured in 96-well plates and UVC-irradiated (20 J/m²; +UV) or mock-treated (−UV), followed by 4 h incubation with medium supplemented with 5 μM EdU. Cells were processed as described in (A). Circles and dashed circles indicate non-S-phase and S-phase cells, respectively. (C) Effects of EdU concentration: 48BR cells were UVC-irradiated (20 J/m²), followed by 4 h incubation in media supplemented with various concentrations of EdU (2.5–20 μM). Cells were processed as described in (A). (D) Effects of FdU and fixation process on the UDS assay. 48BR cells were UVC-irradiated (0–40 J/m²), followed by 4 h incubation in media supplemented with 10 μM EdU, and with or without 1 μM FdU. Cells were then fixed with two different protocols. (E) Effects of UV-dose and EdU incubation time-period for the UDS assay. 48BR cells were UVC-irradiated at the indicated doses, followed by incubation in media supplemented with 5 μM EdU for different time-periods (0.5–4 h). Cells were processed as described in (A). Bars or data points, and error bars indicate average fluorescent intensity of discrete nuclei and standard errors, respectively.

As CS cells are only compromised in the TCR pathway of NER, a UDS-deficiency has not been detected by conventional procedures. Fig. 2H and Supplemental Fig. S1 indicate modest but statistically significant UDS reductions in CS-A and CS-B cells, indicating that the automated system may be able to detect minor UDS-deficiencies because of improved objectivity and reproducibility. It may however transpire that, with a broader range of normal and CS cell-lines, these variable UDS reductions in CS cell-lines may in fact fall within the normal range; nevertheless, the system is at least sensitive enough to detect cell line-to-cell line UDS variations, consistently.

Please cite this article in press as: Y. Nakazawa, et al., A semi-automated non-radioactive system for measuring recovery of RNA synthesis and unscheduled DNA synthesis using ethynyluracil derivatives, DNA Repair (2010), doi:10.1016/j.dnarep.2010.01.015

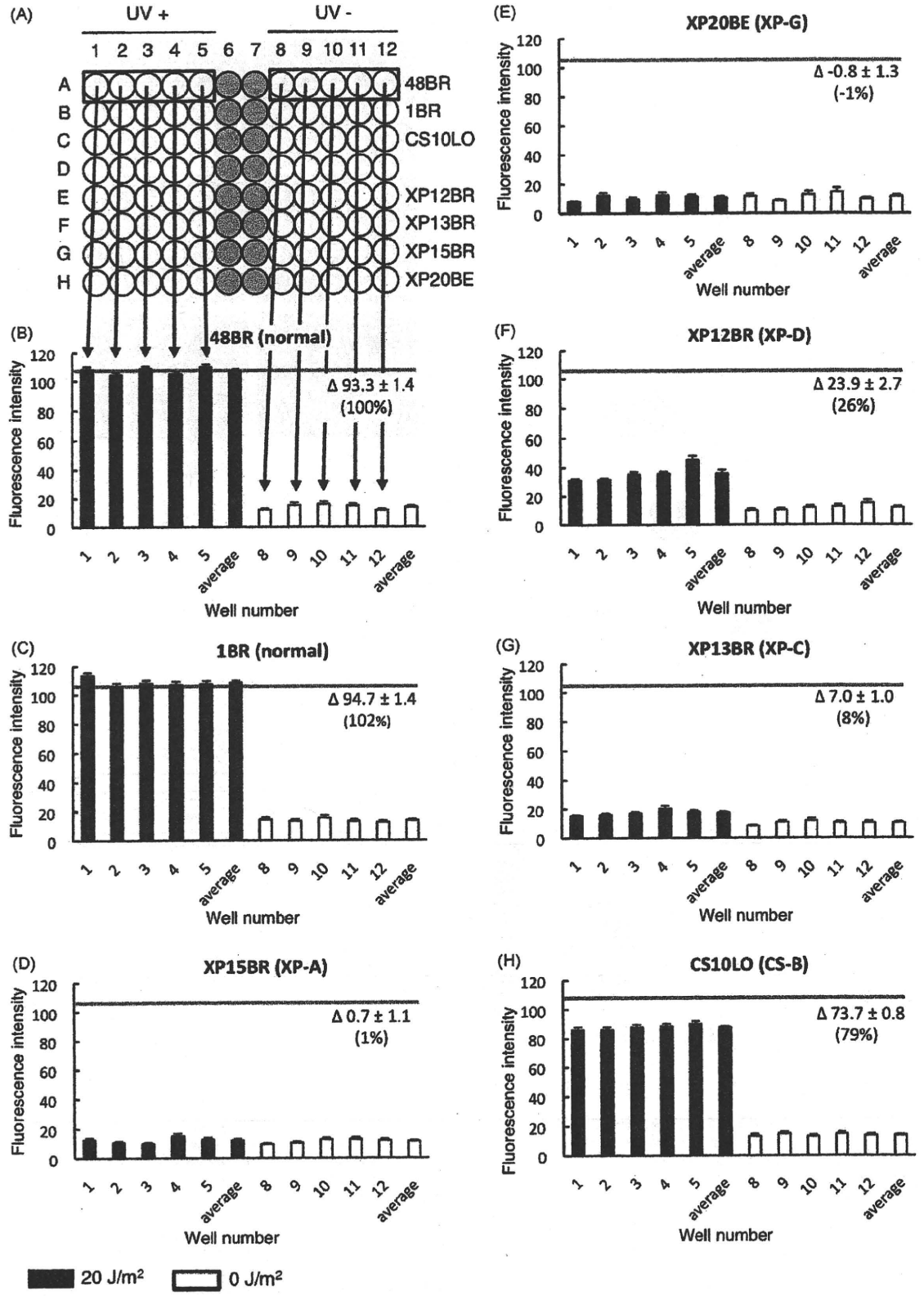

Fig. 2. Reproducible detection of NER-activity by the UDS assay system. (A) The EdU-based UDS assay on normal and NER-deficient fibroblasts was performed together in a single 96-well plate. (B–H) The indicated human primary fibroblasts were seeded in a 96-well plate in quintuplicate as shown in (A). The assay plate was half-covered by a plastic-board wrapped in aluminum foil and UVC-irradiated (closed bars, 20 J/m²; open bars, no-UV), followed by 4 h incubation with media supplemented with 5 μM EdU. Cells were then processed as described in Fig. 1. Bars and error bars indicate average fluorescent intensity of discrete nuclei and standard errors, respectively. Δ represents UDS difference between irradiated and unirradiated samples. Percentages indicate UDS levels normalised against 48BR (red lines). Student's *t*-test was performed to evaluate differences in UDS levels between cell lines: 48BR vs. 1BR, not significant ($p = 0.5$); XP15BR vs. XP20BE, not significant ($p = 0.3$); 48BR vs. CS10LO, CS10LO vs. XP12BR, XP15BR vs. XP13BR and XP12BR vs. XP13BR, significant ($p < 0.01$). (For interpretation of the references to color in this figure legend, the reader is referred to the web version of the article.)

Please cite this article in press as: Y. Nakazawa, et al., A semi-automated non-radioactive system for measuring recovery of RNA synthesis and unscheduled DNA synthesis using ethynyluracil derivatives, DNA Repair (2010), doi:10.1016/j.dnarep.2010.01.015

The UDS levels that we have measured were in good agreement with the levels assayed by thymidine incorporation and with our EdU based measurements on coverslips (Supplemental Table S1) [13], indicating that the system provides a convenient, but sensitive and accurate assay for UDS.

3.3. EU-based non-radioactive recovery of RNA synthesis (RRS) assay using In-Cell-Analyzer

After our recent publication, we noticed that EU, which can be used for *in vivo* RNA-labeling, had become commercially available (*Invitrogen*). We assumed that an EU-based RRS assay might be a good alternative for the classical radioisotope based assays. As an EU-based RNA-labeling protocol has been recently published [15], we tested if EU incorporation could be used to detect the delay in RNA synthesis recovery typical of TCR-deficient CS fibroblasts, and whether it can be assessed on the automated system (scheme described in Fig. 3A). In normal fibroblasts, we could detect EU incorporation-specific fluorescence signals over the EU concentration range we examined; this incorporation was significantly inhibited by UV-irradiation (Fig. 3B). Unlike in the case of EdU labeling, permeabilisation procedures did not influence the fluorescence levels (data not shown). We found that, with our improved coupling protocol described in detail in Section 2, a 2 h labeling period with 100 μM EU was sufficient for RNA synthesis detection in normal 48BR cells without DNA damaging treatment (Fig. 3C and D), even though the original publication noted that a higher EU concentration and longer incubation period are optimum for the EU labeling [15]. (We also noted that the EU labeling efficiency did not increase linearly with incubation time (Fig. 3D).) We then examined RNA synthesis recovery after UVC-irradiation (Fig. 3E). For CS diagnostic tests, a typical protocol measures RNA synthesis levels 16–24 h after irradiation of samples with different UV-doses [21]. As shown in Fig. 3E, using the automated EU assay, RNA synthesis recovers after a few hours in response to UV in normal fibroblasts, while in CS-B cells (CS1OLO), no significant recovery was observed even 24 h after irradiation with UV-doses of 10 J/m^2 and above. However, we decided to use 5 J/m^2 UVC-irradiation and 4 h recovery for the RRS assay in the system, as the shorter recovery period diminishes the time needed for the assay, and this condition provided good discrimination between normal and CS cells. Although increased discrimination could be obtained with longer recovery times, we chose to use this short recovery protocol, so that we can complete a set of UDS and RRS assays in a single day. CS cell-lines were assayed using this system and statistically significant reductions in RRS were clearly detected, while almost complete RNA synthesis recovery was observed in normal fibroblasts (Fig. 4A–D, and Supplemental Figure S2). We also detected reduced recovery in TCR-defective XP-A (XP15BR) and XP-D (XP12BR) cells (Fig. 4E and F), while recovery in two XP-C cells, XP13BR (mild UDS-deficiency) and XP21BR (severe UDS-deficiency), which are compromised in GGR but not TCR, approached that in normal controls (Fig. 4G and H). These results reflect those obtained with conventional assays (e.g. [10]) and demonstrate that the EU-based RRS assay in conjunction with the *In-Cell-Analyzer* provides a convenient and accurate measurement of RNA synthesis recovery, and is suitable for rapid diagnoses of TCR-compromised disorders.

3.4. Rapid UDS measurements for lymphoblastoid cells provided by the EdU-based assay

We further tested whether the EdU-based UDS assay might also be applicable to peripheral lymphocyte samples: lymphocyte-based diagnoses would be less invasive than existing assays that require fibroblasts from skin-biopsies. B-cell enriched lymphocytes can be prepared from whole-blood samples by use of immuno-magnetic-beads as well as Ficoll-based separation reagents. As a first step towards analyses using lymphocytes, we performed EdU-based UDS assays on EBV-immortalised lymphoblastoid cell lines (LCLs) established from normal donors (277, and 701), and from XP-patients (XPL5, XP-V; XPL15OS, XP-A) using the experimental scheme shown in Fig. 5A. LCLs were cultured for 72 h in low-serum media to diminish the number of cells in S-phase. Cells were then UVC irradiated (20 J/m^2), followed by 1 h incubation in serum-free medium supplemented with 10 μM EdU (experimental details described in Section 2). UV-induced UDS was detected in normal 277 and 701 LCLs (Fig. 5B and C), while no detectable UDS was observed in XP-A deficient XPL15OS (Fig. 5D). As expected, we observed normal UDS levels in the XP variant XPL5 cells (Fig. 5E). These results confirm that the EdU-based UDS assay might be applicable for XP diagnosis with clinical blood samples.

3.5. A potential use of the automated system for large scale screens

A major advantage of using automated systems is that they can be used for large-scale screens. We considered if our set-up might be applicable to searching for novel genes in NER using an siRNA-based screen. To test the system, we designed a small-scale pilot experiment knocking-down XP and genes unrelated to NER using a set of siRNA oligos. 48BR cells were transfected with siRNA in 96-well plates, and UDS and RRS levels were measured by the system (Fig. 6A; details of RNA interference are described in Section 2). As expected, we detected a reduction in UDS and RRS in the cells transfected with XP-targeting siRNAs, whereas it remained unchanged in cells transfected with either control siRNA or siRNAs against NER-unrelated genes (Fig. 6B and C). Note that no attempt was made in this pilot study to optimize knockdown conditions. As siRNA-based gene targeting is often imperfect, screening systems have to be sensitive and reproducible enough to pick-up small changes in NER activity. Our system is sensitive enough to detect the effects of knocking-down known XP genes, suggesting that it can be used for an extensive screen.

4. Discussion

The most commonly used techniques for UDS and RRS measurements involve ^{3}H-thymidine labeled nucleoside incorporation, followed by evaluation of silver-grain counting after autoradiography of tissue-culture coverslips [9]. Since it is both accurate and sensitive, this laborious technique has remained in vogue even after several alternative methods have been reported [12,21–23]. Bromodeoxyuridine (BrdU) and bromouridine (BU) are respectively popular alternatives for DNA-labeling by ^{3}H-thymidine and RNA-labeling by ^{3}H-uridine. Nevertheless publications using BrdU for UDS and BU for RRS assays have been very limited due to their restricted sensitivity and resolution [22,24]. Recently developed alkyne-conjugated nucleoside analogues, EdU and EU, have been proved to be useful for S-phase DNA labeling and detection of nascent RNA synthesis, respectively [14,15]; however it has not been clear whether labeling with these nucleoside analogues was sufficiently robust to enable their use in UDS and RRS. In our preceding report, we demonstrated that an EdU-based UDS assay is accurate enough to be an alternative to autoradiography [13]; the biggest improvements from employing EdU to the UDS assay are the obviation of the need to use radioactive materials, and of time-consuming and skilled procedures. We showed in our report, that the entire UDS assay can be completed within a day from preparation of the assay coverslips, and also that the method is compatible with standard cell-biology techniques such as immunofluorescent

Please cite this article in press as: Y. Nakazawa, et al., A semi-automated non-radioactive system for measuring recovery of RNA synthesis and unscheduled DNA synthesis using ethynyluracil derivatives, DNA Repair (2010), doi:10.1016/j.dnarep.2010.01.015

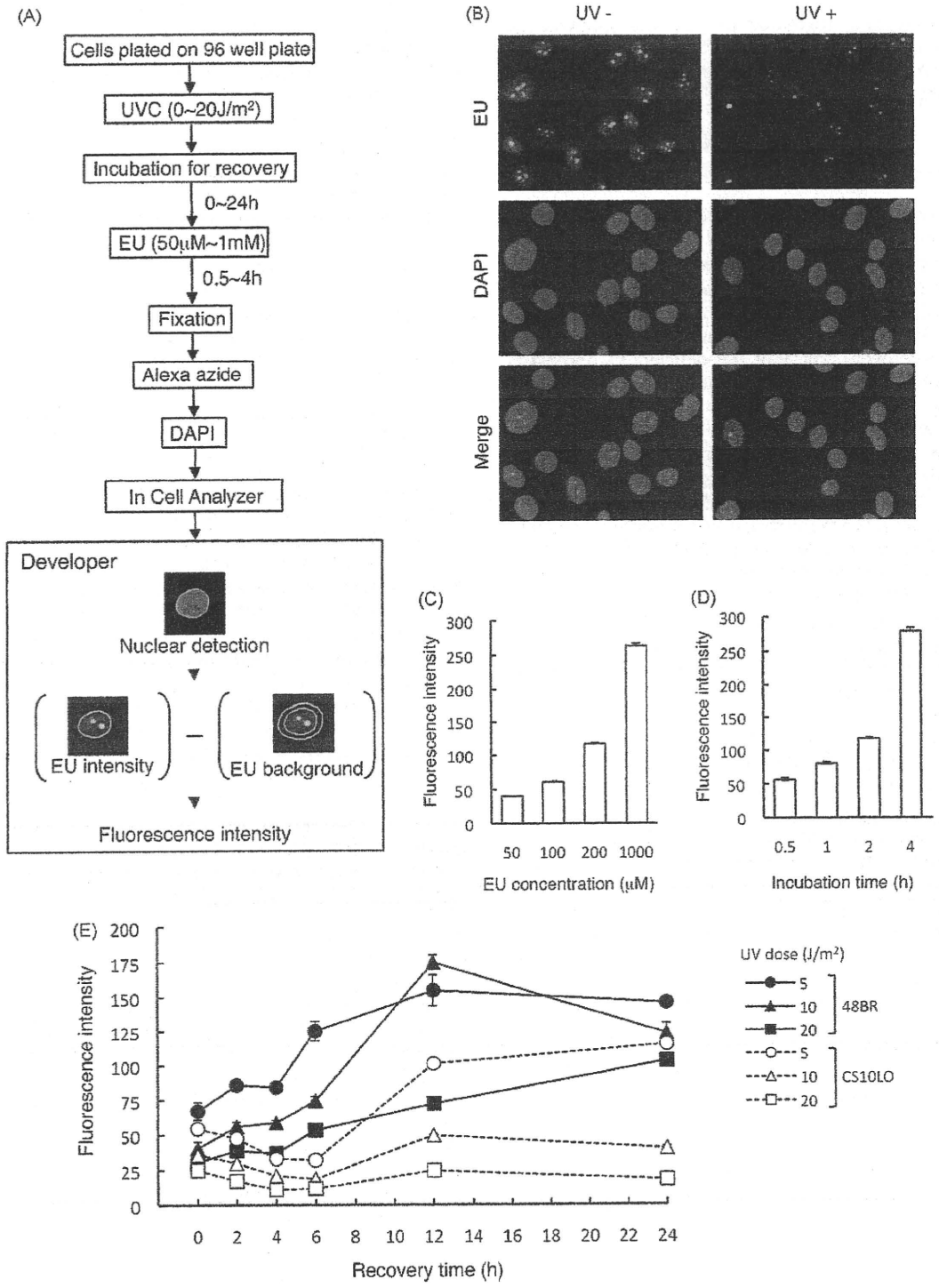

Fig. 3. EU-based semi-automated RRS assay using *In-Cell-Analyzer*. (A) An experimental scheme of the RRS assay. Cells were plated on plastic 96-well plates, UVC-irradiated with a range of doses (0–20 J/m²), followed by incubation for different time-periods (0–24 h) for RNA synthesis recovery in media supplemented with 1% FCS. Cells were then incubated for different time-periods (0.5–4 h) with serum-free media supplemented with various concentrations of EU (50–1000 μM). Incorporated EU was detected as described in Section 2. Image acquisition and data processing were automated using the automated system. (B) Typical RNA synthesis images captured by the *In-Cell-Analyzer*. Normal 48BR cells were cultured in 96-well plates and UVC-irradiated (5 J/m²; +UV) or mock-treated (−UV). Cells were then incubated for 2 h for RNA-labeling with serum-free media supplemented with 100 μM EU. (C) Effect of EU concentration on RNA-labeling. 48BR cells were incubated for 2 h in media supplemented with various concentrations of EU (50–1000 μM). (D) Effect of incubation time on RNA-labeling. 48BR cells were incubated for different time-periods in media supplemented with 100 μM EU. (E) Effects of UV-dose and RNA synthesis recovery time-period for the RRS assay. Normal 48BR (closed symbols) and CS-patient-derived CS10LO (open symbols) cells were UVC-irradiated at the indicated doses (5–20 J/m²), followed by incubation for different time-periods (0–24 h) in media supplemented with 1% FCS to allow RNA synthesis recovery. Subsequently, RNA was labeled for 2 h in a serum-free medium supplemented with 100 μM EU. Bars or data points, and error bars indicate average fluorescent intensity of discrete nuclei and standard errors, respectively.

Please cite this article in press as: Y. Nakazawa, et al., A semi-automated non-radioactive system for measuring recovery of RNA synthesis and unscheduled DNA synthesis using ethynyluracil derivatives, DNA Repair (2010), doi:10.1016/j.dnarep.2010.01.015

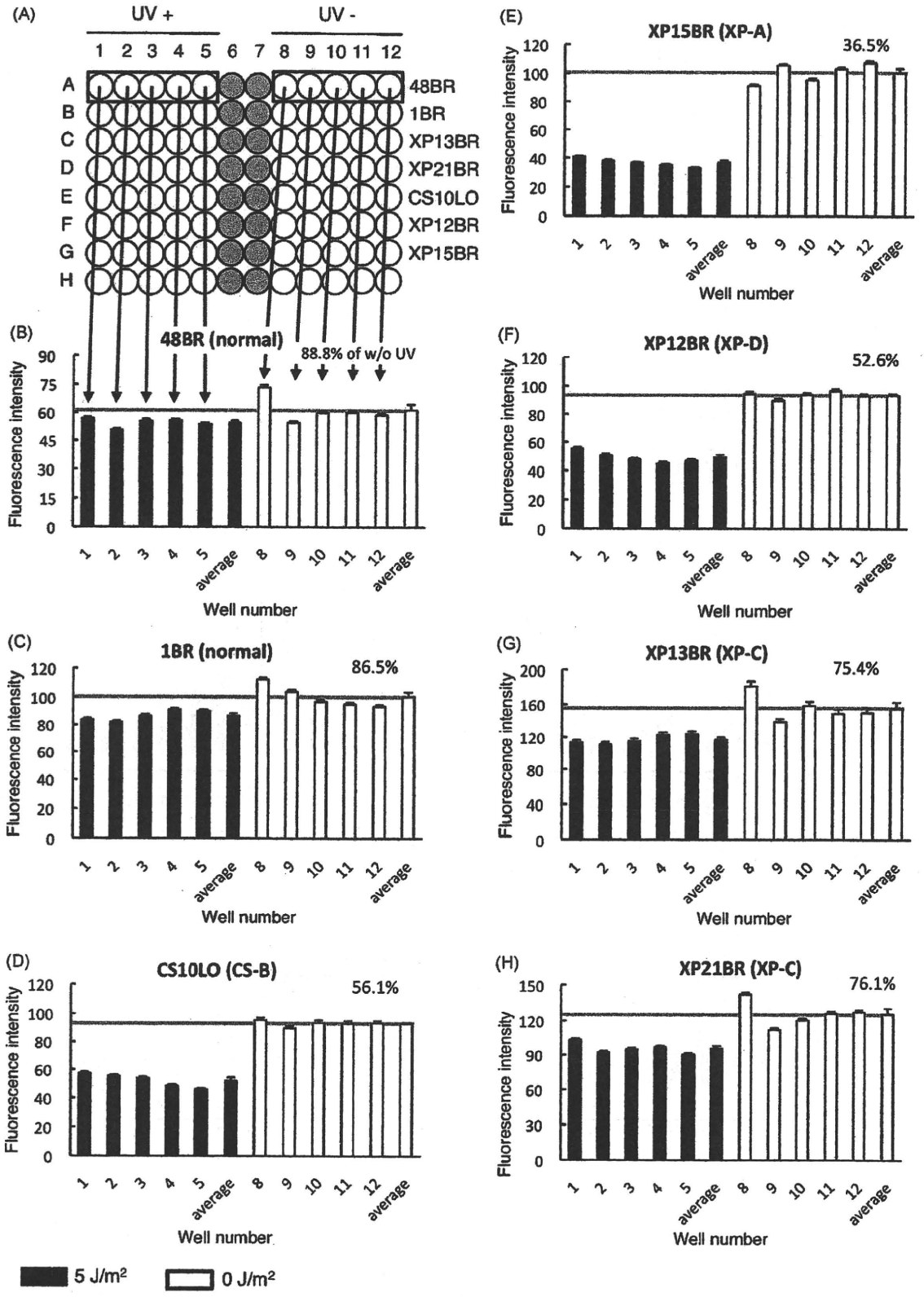

Fig. 4. EU-based semi-automated RRS assay distinguishes between GGR and TCR -compromised XP cells. (A) EU-based RNA synthesis recovery assay on normal and NER-deficient fibroblasts were performed at once in a single 96-well plate. (B–H) The indicated human primary fibroblasts were seeded into a 96-well plate in quintuplicate and UVC-irradiated (closed bars, 5 J/m²; open bars, no-UV) as described in Fig. 2. The cells were incubated for 4 h in media supplemented with 1% FCS to allow RNA synthesis recovery, followed by RNA-labeling for 2 h in a serum-free medium supplemented with 100 μM EU. Cells were then processed as described in Fig. 3. Bars or data points, and error bars indicate average fluorescent intensity of discrete nuclei and standard errors, respectively. RRS levels were normalised and expressed as percentages of the average RNA synthesis levels in unirradiated cells (red lines). Student's *t*-test was performed to evaluate differences in RRS levels between cell lines: 48BR vs. 1BR, not significant ($p = 0.2$); XP13BR vs. XP21BR, not significant ($p = 0.8$); 48BR vs. CS10LO, 48BR vs. XP21BR and XP21BR vs. CS10LO, significant ($p < 0.01$). (For interpretation of the references to color in this figure legend, the reader is referred to the web version of the article.)

Please cite this article in press as: Y. Nakazawa, et al., A semi-automated non-radioactive system for measuring recovery of RNA synthesis and unscheduled DNA synthesis using ethynyluracil derivatives, DNA Repair (2010), doi:10.1016/j.dnarep.2010.01.015

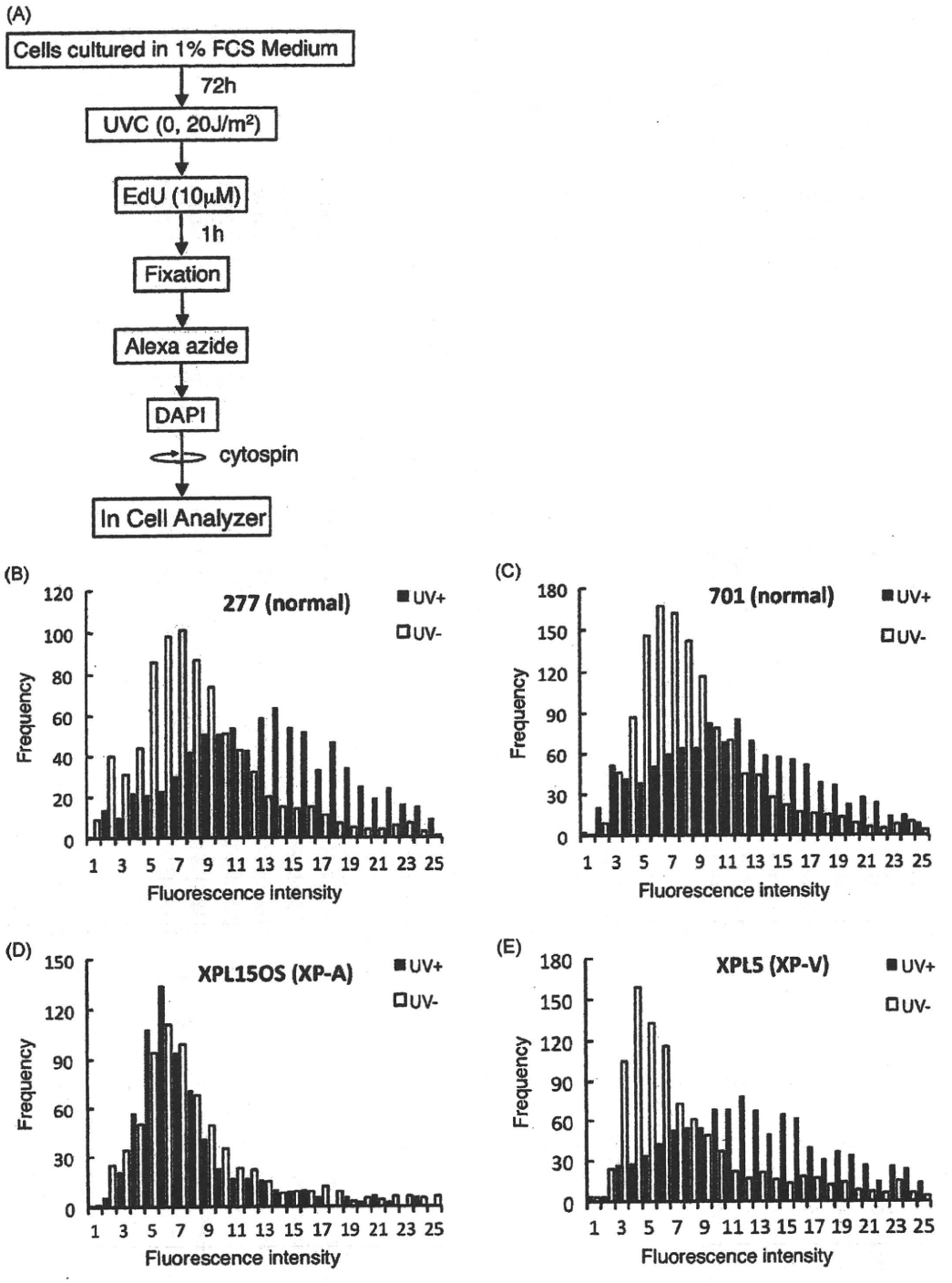

Fig. 5. UDS assayed in normal and XP-patient derived lymphoblastoid samples. (A) An experimental scheme of the UDS assay for lymphoblastoid samples. Lymphoblastoid cells were cultured for 72 h in low-serum media to diminish the number of cells in S-phase. Cells were then UVC-irradiated (20 J/m^2), followed by 1 h incubation in serum-free medium supplemented with 10 μM EdU. Cells were then fixed and permeabilised, and processed as detailed in Section 2. The azide-coupling reaction was performed in eppendorf tubes. Processed cells were then cytospin-centrifuged, and images captured and analysed by the *In-Cell-Analyzer*. (B–E) Lymphoblastoid cells derived from normal, and XP-patients were assayed by the system. Histograms of the UDS assay with irradiated (closed bars) and unirradiated (open bars) cells are shown.

staining and labeling of cells with micro-latex beads, which are often used in combination with the UDS assay.

In this report, we firstly automated the UDS assay. This approach dramatically improved the sensitivity of the EdU-based method; the system achieved more than ~50% reduction of the background signals (compare Ref. [13] and Fig. 2), which is now as good as the conventional autoradiographic technique [9]. The assay is sensitive and reproducible enough to distinguish between normal controls and TCR-deficient CS cells, as well as between severely UDS-deficient XP-A or XP-G cells and moderately deficient XP-D or XP-C cells (Fig. 2B–H, and Supplemental Fig. S1). Secondly, we adopted an RNA precursor, EU, which has recently become commercially available, for the RRS assay. The EU-based RRS assay is also suitable for use in the automated system. Both UDS and RRS levels can be measured in 96-well plates as sensitively as using autoradiography. We finally evaluated the system for several appli-

Please cite this article in press as: Y. Nakazawa, et al., A semi-automated non-radioactive system for measuring recovery of RNA synthesis and unscheduled DNA synthesis using ethynyluracil derivatives, DNA Repair (2010), doi:10.1016/j.dnarep.2010.01.015

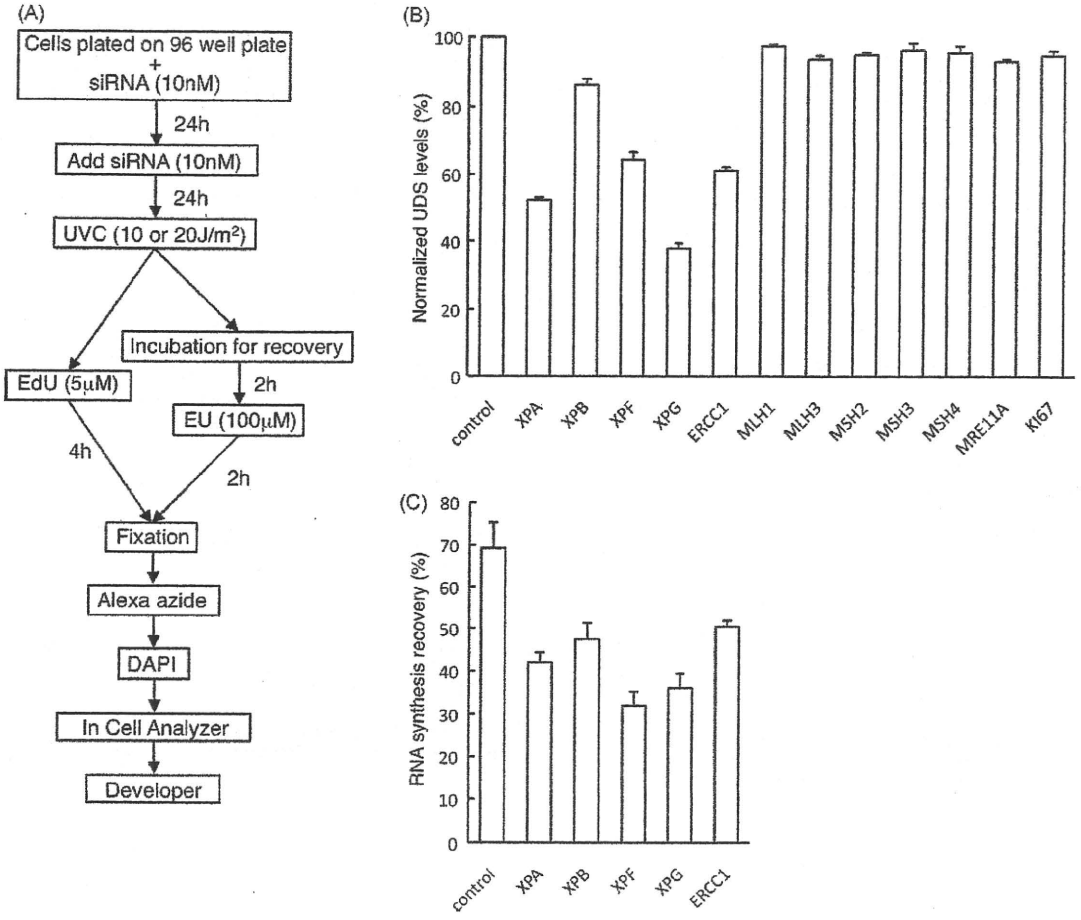

Fig. 6. A pilot experiment for prospective siRNA-screening performed by the automated system. (A) Experimental scheme of the siRNA transfection and subsequent NER-activity assayed by the automated system. (B and C) Cells were transfected with indicated siRNAs prior to UV-irradiation, and NER-activity was measured as described in (A). (B) UDS activities in cells depleted for XP and NER-unrelated genes. UDS activity was normalised against samples which were transfected with non-targeting control siRNA. (C) RRS activities in cells depleted for XP genes. RNA synthesis recovery levels were normalised against the RNA synthesis levels in unirradiated cells. Error bars indicate standard errors of means of measurements in triplicate wells.

cations. We showed that the EdU-based UDS assay is applicable to lymphoblast samples. Although the results are not as precise as with fibroblasts, this blood-sample-based approach may eventually benefit the patients as it obviates invasive skin-biopsies.

We also investigated the suitability of the system for large-scale screening. We designed a pilot siRNA-screening experiment; it demonstrated that a microtiter plate-based NER-activity assay can be used for screening. The automated NER-assay system can process ~twenty 96-well plates per day (*In-Cell-Analyzer 1000*). This enables the evaluation of both UDS and RRS activities of ~100 different samples to be carried out in a day, if the screening is performed using the format shown in Figs. 2A and 4A. The above EdU or EU -based assays can be transferred to a commonly used fluorescent microscope equipped with a motorised stage and focus, and a monochrome CCD camera. We have set-up a system using a Zeiss microscope, Axio-Observer Z1, equipped with a long working distance lens, HRm monochrome CCD camera, and an ASI's motorised X–Y stage, MS-2000. Sequential image acquisition and analysis are performed automatically on a macroprogram running Axiovision software (the script is available from the authors).

The NER-deficiency assessments by incorporation measurements of EdU and EU have the potential to become standard techniques in basic NER research as well as in clinical diagnosis of NER-related diseases. They also have the potential for use in chemotherapy, for example to measure NER in tumor cells to predict sensitivity to platinum-based therapy.

Conflict of interest

None.

Acknowledgements

We are grateful to Heather Fawcett for technical assistance. This work was supported by a Grant in aid for Honeybee Research from Yamada Apiculture Center Inc., a research grant from ROHTO Pharmaceutical Co., Ltd., Special Coordination Funds for Promoting Science and Technology from Japan Science and Technology Agency (JST), a Grant in aid for Seeds Innovation (Type-A) from JST, a Grant in aid for Scientific Research KAKENHI (20810021) from Japan Society for the Promotion of Science (JSPS) to T.O.; a Grant in aid for Scientific Research KAKENHI (21810022) from JSPS to Y.N.; a Global COE Program from the Ministry of Education, Culture, Sports, Sciences and Technology of Japan to T.O., Y.N. and S.Y. CS-patient-derived CS16PV and CS20PV are kind gifts from Dr. Miria Stefanini (Pavia).

Appendix A. Supplementary data

Supplementary data associated with this article can be found, in the online version, at doi:10.1016/j.dnarep.2010.01.015.

Please cite this article in press as: Y. Nakazawa, et al., A semi-automated non-radioactive system for measuring recovery of RNA synthesis and unscheduled DNA synthesis using ethynyluracil derivatives, DNA Repair (2010), doi:10.1016/j.dnarep.2010.01.015

References

[1] E.C. Friedberg, G.C. Walker, W. Siede, R.D. Wood, R.A. Schultz, T. Ellenberger, DNA Repair and Mutagenesis, 2nd ed., ASM Press, 2005.
[2] K.H. Kraemer, N.J. Patronas, R. Schiffmann, B.P. Brooks, D. Tamura, J.J. DiGiovanna, Xeroderma pigmentosum, trichothiodystrophy and Cockayne syndrome: a complex genotype-phenotype relationship, Neuroscience 145 (2007) 1388–1396.
[3] A.R. Lehmann, DNA repair-deficient diseases, xeroderma pigmentosum, Cockayne syndrome and trichothiodystrophy, Biochimie 85 (2003) 1101–1111.
[4] J.E. Cleaver, Cancer in xeroderma pigmentosum and related disorders of DNA repair, Nat. Rev. Cancer 5 (2005) 564–573.
[5] S.C. Shuck, E.A. Short, J.J. Turchi, Eukaryotic nucleotide excision repair: from understanding mechanisms to influencing biology, Cell Res. 18 (2008) 64–72.
[6] D. Bootsma, K.H. Kraemer, J.E. Cleaver, J.H. Hoeijmakers, Nucleotide excision repair syndromes: xeroderma pigmentosum, Cockayne syndrome and Trichothiodystrophy, in: C.R. Scriver, A.L. Beaudet, W.S. Sly, D. Valle (Eds.), The Metabolic and Molecular Bases of Inherited Disease, 8th ed., McGraw-Hill, New York, 2001, pp. 677–703.
[7] L.C. Gillet, O.D. Scharer, Molecular mechanisms of mammalian global genome nucleotide excision repair, Chem. Rev. 106 (2006) 253–276.
[8] P.C. Hanawalt, G. Spivak, Transcription-coupled DNA repair: two decades of progress and surprises, Nat. Rev. Mol. Cell. Biol. 9 (2008) 958–970.
[9] M. Stefanini, P. Lagomarsini, S. Giliani, T. Nardo, E. Botta, A. Peserico, W.J. Kleijer, A.R. Lehmann, A. Sarasin, Genetic heterogeneity of the excision repair defect associated with trichothiodystrophy, Carcinogenesis 14 (1993) 1101–1105.
[10] L.V. Mayne, A.R. Lehmann, Failure of RNA synthesis to recover after UV irradiation: an early defect in cells from individuals with Cockayne's syndrome and xeroderma pigmentosum, Cancer Res. 42 (1982) 1473–1478.
[11] C. Masutani, R. Kusumoto, A. Yamada, N. Dohmae, M. Yokoi, M. Yuasa, M. Araki, S. Iwai, K. Takio, F. Hanaoka, The XPV (xeroderma pigmentosum variant) gene encodes human DNA polymerase eta, Nature 399 (1999) 700–704.
[12] A.R. Lehmann, S. Stevens, A rapid procedure for measurement of DNA repair in human fibroblasts and for complementation analysis of xeroderma pigmentosum cells, Mutat. Res. 69 (1980) 177–190.
[13] S. Limsirichaikul, A. Niimi, H. Fawcett, A. Lehmann, S. Yamashita, T. Ogi, A rapid non-radioactive technique for measurement of repair synthesis in primary human fibroblasts by incorporation of ethynyl deoxyuridine (EdU), Nucleic Acids Res. 37 (2009) e31.
[14] A. Salic, T.J. Mitchison, A chemical method for fast and sensitive detection of DNA synthesis in vivo, Proc. Natl. Acad. Sci. U.S.A. 105 (2008) 2415–2420.
[15] C.Y. Jao, A. Salic, Exploring RNA transcription and turnover in vivo by using click chemistry, Proc. Natl. Acad. Sci. U.S.A. 105 (2008) 15779–15784.
[16] C.F. Arlett, M.H. Green, A. Priestley, S.A. Harcourt, L.V. Mayne, Comparative human cellular radiosensitivity: I. The effect of SV40 transformation and immortalisation on the gamma-irradiation survival of skin derived fibroblasts from normal individuals and from ataxia-telangiectasia patients and heterozygotes, Int. J. Radiat. Biol. 54 (1988) 911–928.
[17] C.F. Arlett, P.N. Plowman, P.B. Rogers, C.N. Parris, F. Abbaszadeh, M.H. Green, T.J. McMillan, C. Bush, N. Foray, A.R. Lehmann, Clinical and cellular ionizing radiation sensitivity in a patient with xeroderma pigmentosum, Br. J. Radiol. 79 (2006) 510–517.
[18] S. Moriwaki, M. Stefanini, A.R. Lehmann, J.H. Hoeijmakers, J.H. Robbins, I. Rapin, E. Botta, B. Tanganelli, W. Vermeulen, B.C. Broughton, K.H. Kraemer, DNA repair and ultraviolet mutagenesis in cells from a new patient with xeroderma pigmentosum group G and cockayne syndrome resemble xeroderma pigmentosum cells, J. Invest. Dermatol. 107 (1996) 647–653.
[19] D.L. Mallery, B. Tanganelli, S. Colella, H. Steingrimsdottir, A.J. van Gool, C. Troelstra, M. Stefanini, A.R. Lehmann, Molecular analysis of mutations in the CSB (ERCC6) gene in patients with Cockayne syndrome, Am. J. Hum. Genet. 62 (1998) 77–85.
[20] H. Tohda, A. Oikawa, T. Katsuki, Y. Hinuma, M. Seiji, A convenient method of establishing permanent lines of xeroderma pigmentosum cells, Cancer Res. 38 (1978) 253–256.
[21] A.R. Lehmann, A.F. Thompson, S.A. Harcourt, M. Stefanini, P.G. Norris, Cockayne's syndrome: correlation of clinical features with cellular sensitivity of RNA synthesis to UV irradiation, J. Med. Genet. 30 (1993) 679–682.
[22] B.F. Droy, M.R. Miller, T.M. Freeland, D.E. Hinton, Immunohistochemical detection of CCl4-induced, mitosis-related DNA synthesis in livers of trout and rat, Aquat. Toxicol. 13 (1988) 155–166.
[23] F. Vincent, J. Ceraline, S. Goldblum, C. Klein-Soyer, J.P. Bergerat, A new flow cytometric method to follow DNA gap filling during nucleotide excision repair of UVc-induced damage, Cytometry 45 (2001) 96–101.
[24] S. Hashimoto, K. Egawa, H. Ihn, S. Tateishi, Non-radioisotope method for diagnosing photosensitive genodermatoses and a new marker for xeroderma pigmentosum variant, J. Dermatol. 36 (2009) 138–143.

Please cite this article in press as: Y. Nakazawa, et al., A semi-automated non-radioactive system for measuring recovery of RNA synthesis and unscheduled DNA synthesis using ethynyluracil derivatives, DNA Repair (2010), doi:10.1016/j.dnarep.2010.01.015

2. 麻酔と心機能

澄川耕二
長崎大学大学院医歯薬学総合研究科　麻酔・蘇生科学分野

最近の動向

不整脈に関して術前心電図検査の意義が検討された．心リスク因子のない患者では心電図異常の頻度は0.44%程度にすぎず，術前検査の意義は限られるようである．手術と心機能に関しては，予後に影響する因子や予後予測因子の探索が盛んである．非心臓手術では術前のBNP，高血糖，左室拡張障害などが予後との関連で注目され，心臓手術では左室機能低下が予後に影響するという．一方，予後を改善する因子としてスタチンが注目される．プレコンディショニングに関しては，揮発性麻酔薬の基礎および臨床的検討が続いており，さらに硫化水素やヘリウムなど新たなガスの心保護作用も見いだされている．

不整脈と心臓電気生理

レミフェンタニルは徐脈性不整脈を生じることが知られている．ブタで電気生理学的作用を調べたところ，洞結節機能（洞結節回復時間，洞房伝道時間）と房室結節機能（AH伝導時間）を抑制し，His-Purkinje機能と心室内伝導には影響しなかった．この洞結節と房室結節への抑制作用が徐脈を生じる原因とみられる[1]．

心電図のQT延長は再分極過程の異常であるが，薬剤によっても生じることがあり，トルサード・ド・ポアンツとも関連している．T波のピークから終わりまでの時間（Tp-e）は心室壁の再分極のばらつきを表し，重症度を反映する．3～10歳の小児でプロポフォールTCIの影響を調べたところ，TCI濃度3，4.5，6 μg/mLのいずれでもQTcとTp-eは変化しなかった．再分極過程に異常を有する小児においても，プロポフォールの使用は問題ないと思われる[2]．

虚血性不整脈に対する麻酔薬の影響をみるため，ラットで冠動脈を30分間閉塞し生存率を調べた．コントロールの生存率83%に比べ，プロポフォール麻酔ラットでは94%，セボフルラン麻酔ラットでは67%であった．プロポフォール麻酔ラットではconnexin43がよく保存されており，これが重篤不整脈を抑制する機序かもしれない．Connexin43は心ギャップジャンクションチャ

1) Zaballos M, Jimeno C, Almendral J et al：Cardiac electrophysiological effects of remifentanil：study in a closed-chest porcine model. Br J Anaesth 103：191-198, 2009

2) Hume-Smith HV, Sanatani S, Lim J et al：The effect of propofol concentration on dispersion of myocardial repolarization in children. Anesth Analg 107：806-810, 2008

麻酔科学レビュー　2010
1884-8516/10/¥400/論文/JCOPY

ネル蛋白で，虚血により減少するため不整脈が生じやすくなるとみられている[3]．

心臓のリスクファクターをもたない患者では，術前心電図異常は存在しないはずという仮説が検証された．**術前患者1149名中89名が重大な心電図異常を呈し，そのほとんどがリスクファクターを有していた．リスクファクターは65歳以上の年齢，心不全，狭心症，心筋梗塞などであった．リスクファクターをもたない患者でも心電図異常は存在し，その頻度は0.44%であった．**これは，リスクファクターをもたない患者で術前心電図検査を省略した場合，手術室で初めて発見され手術が中止される頻度がこの程度ということを意味する．すなわち，リスクファクターのないことを確実に識別できれば，術前心電図検査は省いてもよいであろう[4]．

ペースメーカー装着患者にみられた術中の予期せぬレート変化について，症例報告があった．DOOモードで70/minに設定された患者に麻酔を施行したところ，レートが急に50/minに減少し，3分で元に戻った．このようなことが術中何度か起こり，ペースメーカーの機能異常と思われた．後で判明したのであるが，比較的新しい機能である休止モード(rest mode)や睡眠モード(sleep mode)が作動すると，このようなペーシングレートの予想しない変化が生じ，麻酔科医が当惑することになる．この新しい機能によるレート設定について，あらかじめ知っておくことが必要である[5]．

非心臓大手術の麻酔と心機能

最近，麻酔と長期予後について関心が高まり，予後予測因子やリスク因子の研究が盛んである．脳性Na利尿ペプチド(BNP)は，心室壁ストレスや虚血に反応して心筋細胞で合成されるホルモンであり，左室機能不全，弁膜症，急性冠症候群などの心病態と関連している．非心臓大手術における術前BNPレベルの予後予測の役割について，15論文のメタ分析を行った．BNPとその前駆物質NT-proBNPの増加は，術後の短期的および長期的心イベントの増加と関連し，そのオッズ比は短期19.7，長期17.7であった．また全原因死亡率も増加し，オッズ比はそれぞれ9.28と4.77であった．BNP増加は，非心臓大手術において術後のハイリスク患者を識別するのに有用であるといえる[6]．

高血糖は，独立した心血管リスクとなることが知られている．非心臓手術において厳密な血糖コントロールが有利であるかどうかを調べた．**末梢血管手術を受ける患者で，インスリンの持続投与で血糖100～150mg/dLに厳密管理する群と，従来の間欠投与で150mg/dL以上に管理する群に分け比較した．術後心イベントまたは全原因死の発生率は，従来の方法で12.3%であったのに比し，厳密管理では3.5%に減少した．厳密な血糖管理が予後を改善するといえよう[7]．**

3) Hirata N, Kanaya N, Kamada N et al : Differential effects of propofol and sevoflurane on ischemia-induced ventricular arrhythmias and phosphorylated connexin 43 protein in rats. Anesthesiology 110 : 50-57, 2009

4) Correll DJ, Hepner DL, Chang C et al : Preoperative electrocardiograms. Anesthesiology 110 : 1217-1222, 2009

5) Streckenbach SC : Intraoperative pacemaker rate changes associated with the rest mode. Anesthesiology 109 : 1137-1139, 2008

6) Ryding ADS, Kumar S, Worthington AM et al : Prognostic value of brain natriuretic peptide in noncardiac surgery. Anesthesiology 111 : 311-319, 2009

7) Subramaniam B, Panzica PJ, Novack V et al : Continuous perioperative insulin infusion decreases major cardiovascular events in patients undergoing vascular surgery. Anesthesiology 110 : 970-977, 2009

非心臓手術における術後30日間の心イベントを予測する術中因子について調べた．7740人の患者の1.1%に術後心イベントが発生した．独立した予後予測因子は，年齢68歳以上，BMI 30以上，緊急手術，冠動脈形成術または心手術の既往，うっ血性心不全の存在，脳血管疾患，高血圧，3.8時間以上の手術，術中輸血，の9つであった．従来の予測因子に術中因子を加えることで，予後予測能力が高まるとみられる[8]．

周術期TEEによる心機能評価と術後合併症との関連について調べた．末梢血管手術患者313名中，収縮障害は8%，拡張障害は43%，収縮拡張障害は24%にみられた．拡張障害は術後うっ血性心不全（発生率20%）と関連していたが，収縮障害は関連していなかった．拡張障害は術後心イベントの予測因子として重視すべきであろう[9]．

腹部大動脈瘤手術の術後は炎症反応と，これに伴う臓器障害が生じることが報告されている．血漿蛋白成分の変化を経時的に調べたところ，術後6時間でトロンビン生成が増加した．この血漿をラット心筋細胞に投与すると収縮機能が抑制され，トロンビン拮抗薬で回復した．炎症反応により生成されるトロンビンが術後の血行動態不安定の原因になることを示唆するものである[10]．

ハイリスクの血管手術患者の周術期心筋虚血を予防する目的で，フォスフォジエステラーゼ（PDE）Ⅲ阻害薬とβ遮断薬を48時間持続投与して効果を調べた．心係数を2.5以上，心拍数を50～60/minにコントロールすることにより，トロポニンT，BNPの上昇が抑制された．ハイリスク患者において有用な方法であろう[11]．

心臓手術の麻酔と心機能

心臓手術においても，予後予測因子とリスク評価に関する研究が進んでいる．トロポニンI，BNP，CRPは急性冠症候群の予後予測因子として知られている．心臓手術の周術期にこれらの血中濃度上昇と予後の関連を調べたところ，心手術後12ヵ月間の心イベント発生のオッズ比は，CRP 2.14，トロポニンI 2.37，BNP 2.65であった．これらは，心臓手術においても長期予後の予測因子といえる[12]．また，CABG術後患者641名のデータを1991年から13年間にわたって追跡して調べた研究では，**術前の左室機能低下と術後腎機能悪化は，いずれも独立した長期死亡率増加の予測因子であり，さらに二つが重複すると死亡リスクは相加的に増える**ことが明らかにされている[13]．左室機能低下の患者が心臓手術後の合併症を生じやすい原因を明らかにするため，CABG手術の術中・術後の全身性炎症反応への影響をが調べられた．駆出率30%以下の患者では，IL6とIL8レベルが術前から術中にかけて有意に高値を呈した．このことは，低左室機能患者が体外循環下にCABG手術を受けると全身性炎症反応がより強く生じることを示している[14]．

8) Kheterpal S, O'Reilly M, Englesbe MJ et al：Preoperative and intraoperative predictors of cardiac adverse events after general, vascular, and urological surgery. Anesthesiology 110：58-66, 2009

9) Matyal R, Hess PE, Subramaniam B et al：Perioperative diastolic dysfunction during vascular surgery and its association with postoperative outcome. J Vasc Surg 50：70-76, 2009

10) Modesti PA, Gamberi T, Bazzini C et al：Response of serum proteome in patients undergoing infrarenal aortic aneurysm repair. Anesthesiology 111：844-854, 2009

11) Suttner S, Boldt J, Mengistu A et al：Influence of continuous perioperative beta-blockade in combination with phosphodiesterase inhibition on haemodynamics and myocardial ischaemia in high-risk vascular surgery patients. Br J Anaesth 102：597-607, 2009

12) Fellahi JL, Hanouz JL, Manach YL et al：Simultaneous measurement of cardiac troponin I, B-type natriuretic peptide, and C-reactive protein for the prediction of long-term cardiac outcome after cardiac surgery. Anesthesiology 111：250-257, 2009

13) Loef BG, Epema AH, Navis G et al：Postoperative renal dysfunction and preoperative left ventricular dysfunction predispose patients to increased long-term mortality after coronary artery bypass graft surgery. Br J Anaesth 102：749-755, 2009

14) Karfis EA, Papadopoulos G, Matsagas M et al：The systemic inflammatory response in coronary artery bypass grafting：what is the role of the very low ejection fraction (EF≤30%)？ J Cardiovasc Surg 49：801-808, 2008

スタチンは心臓手術後の短期および長期死亡率を減少させることが報告されている．1557名のスタチン投与患者の術後経過を非投与患者と比較したところ，**スタチンは術後院内死亡リスクを43%減らし，人工腎への移行を46%減らすことが明らかとなり，その有用性は十分認識されるべきであろう**[15]．またレボシメンダンは心筋細胞内のCa^{2+}を増加させずに収縮機能を高めるため，酸素消費量を増加させずに心拍出量を増やすことが知られている．**駆出率50%以下の3血管CABG手術患者で麻酔導入後から持続投与すると，体外循環からの離脱が容易となり，離脱失敗のオッズ比は0.182と著明な効果がみられた**．左室不全の患者の麻酔には有用な薬剤と思われる[16]．

脊髄くも膜下麻酔と心機能

帝王切開術における脊髄くも膜下麻酔は，著しい血圧低下と心拍出量の減少をきたす．晶質液の予防投与は，速やかな血管外分布により血圧維持にあまり有効ではない．ヒドロキシエチル澱粉液（HES）15mL/kgの麻酔前投与と麻酔同時投与の効果を比べた．低血圧の頻度，血圧の絶対値，フェニレフリン使用量に有意差はなく，胎児のアプガースコアー，臍帯血ガス分析にも差がなかった．すなわち，**膠質液輸液は麻酔同時投与でも有効であることを示している**[17]．

前立腺手術を受ける高齢患者で，脊髄くも膜下麻酔による血行動態変化を防止するのに，晶質液＋膠質液と，晶質液のみの，どちらが有効かについて調べた．何も投与しないコントロール群に比べ，HES 500mL＋生食水500mLを投与した群では心拍出量が増加したが，麻酔に伴う低血圧は防止せず，血圧の低下は生食水500mL投与群と有意差がなかった．膠質液投与の意義はないようである[18]．

麻酔薬プレコンディショニング

揮発性麻酔薬はプレコンディショニング作用を有することが知られている．CABG患者でセボフルランの投与法の影響を，血中トロポニンIを指標に検討した．**セボフルラン1MACを対外循環開始前に5分間吸入しただけでは効果がなく，5分間吸入を5分間隔で2回行うと効果が現れた．このことは，セボフルランのプレコンディショニング作用は臨床的に再現可能であるが，投与方法に依存することを示している**[19]．

虚血プレコンディショニングの最終標的としてミトコンドリア膜透過性遷移孔が有力視されている．イソフルランの作用をラット心筋細胞で検討したところ，イソフルランはCa^{2+}によるミトコンドリア膜透過性遷移孔の開口を遅らせるが，これはミトコンドリアへの直接作用ではなく，細胞質のPKC-εの活性化を介して発現するものとみられる[20]．NOはプレコンディショニング経路

15) Huffmyer JL, Mauermann JW, Thiele RH et al：Preoperative statin administration is associated with lower mortality and decreased need for postoperative hemodialysis in patients undergoing coronary artery bypass graft surgery. J Cardiothorac Vasc Anesth 23：468-473, 2009

16) Eriksson HI, Jalonen JR, Heikkinen LO et al：Levosimendan facilitates weaning from cardiopulmonary bypass in patients undergoing coronary artery bypass grafting with impaired left ventricular function. Ann Thorac Surg 87：448-454, 2009

17) Teoh WHL, Sia ATH：Colloid preload versus coload for spinal anesthesia for cesarean delivery：the effects on maternal cardiac output. Anesth Analg 108：1592-1598, 2009

18) Riesmeier A, Schellhaass A, Boldt J et al：Crystalloid/Colloid versus crystalloid intravascular volume administration before spinal anesthesia in elderly patients：the influence on cardiac output and stroke volume. Anesth Analg 108：650-654, 2009

19) Fräßdorf J, Borowski A, Ebel D et al：Impact of preconditioning protocol on anesthetic-induced cardioprotection in patients having coronary artery bypass surgery. J Thorac Cardiovasc Surg 137：1436-1442, 2009

20) Pravdic D, Sedlic F, Mio Y et al：Anesthetic-induced preconditioning delays opening of mitochondrial permeability transition pore via protein kinase C-ε-mediated pathway. Anesthesiology 111：267-274, 2009

に必須であるが，家兎心で調べたところ，イソフルランは熱ショック蛋白90の活性化を介して血管内皮NO合成酵素を活性化し，心筋梗塞を保護する経路が明らかとなった[21]．

アプロチニンの心臓手術における使用は心保護か有害かについて見解が一致していない．**摘出モルモット心の梗塞モデルで，アプロチニンはセボフルランポストコンディショニングを消失させた．**その機序として，アプロチニンはセボフルランによるAkt，PKC-δ，GSK3βのリン酸化を抑制し，NO産生を減少させることがわかった．これは有害作用を示唆するものであるが，臨床における作用については，さらに検討を要する問題である[22]．

リドカインは抗炎症作用を有し，虚血心を保護することが報告されている．**マウス心筋梗塞モデルでリドカインは梗塞サイズを減少させた．さらに*in vitro*の実験で白血球接着は変化せず，心筋細胞のアポトーシスを減少させた．**このことから，リドカインの保護作用は抗炎症作用ではなく抗アポトーシス作用によるものとみられる[23]．

心保護作用を有する非麻酔ガス

マウスをK^+で心停止させ，8分後に人工呼吸と胸部圧迫で蘇生を始めるというモデルで，蘇生は全マウスで成功したが24時間後の生存率は38％であった．これに対して，**蘇生開始1分前から硫化ナトリウムを静注すると生存率が100％になった．これは，生成された硫化水素がNOS-3を活性化して心保護作用を現し，心機能を改善することによる**とみられる[24]．また家兎の心筋梗塞モデルで，ヘリウムもプレコンディショニング作用を示すが，これにも内皮NOSの活性化によるNO産生が仲介するようである[25]．

21) Amour J, Brzezinska AK, Weihrauch D et al：Role of heat shock protein 90 and endothelial nitric oxide synthase during early anesthetic and ischemic preconditioning. Anesthesiology 110：317-325, 2009

22) Inamura Y, Miyamae M, Sugioka S et al：Aprotinin abolishes sevoflurane postconditioning by inhibiting nitric oxide production and phosphorylation of protein kinase C-δ and glycogen synthase kinase 3β. Anesthesiology 111：1036-1043, 2009

23) Kaczmarek DJ, Herzog C, Larmann J et al：Lidocaine protects from myocardial damage due to ischemia and reperfusion in mice by its antiapoptotic effects. Anesthesiology 110：1041-1049, 2009

24) Minamishita S, Bougaki M, Sips PY et al：Hydrogen sulfide improves survival after cardiac arrest and cardiopulmonary resuscitation via a nitric oxide synthase 3-dependent mechanism in mice. Circulation 120：888-896, 2009

25) Pagel PS, Krolikowski JG, Pratt Jr PF et al：The mechanism of helium-induced preconditioning：A direct role for nitric oxide in rabbits. Anesth Analg 107：762-768, 2008